MECHANICS AND CONTROL
Vol. 32 No. 2 2013 http://dx.doi.org/10.7494/mech.2013.32.2.60

Dariusz Grzybek*

LQR CONTROL OF THE NODAL DISPLACEMENTS IN A SPATIAL TRUSS WITH ACTIVE PIEZOELECTRIC MEMBERS

SUMMARY

The ability to damp vibrations is important in many structures, in which trusses are one of the main elements. The increase of the damping of the truss vibrations is possible by passive means or by the use of an active vibration control system integrated with the structure of the truss. The control system can affect the truss structure by specially designed actuators, which generate active forces in appropriate nodes of the truss. Piezoelectrics can be used to build such actuators. The design of the control system encompasses the structure of the actuating active truss member, the spacing of active members inside the truss structure, the design of the control algorithm and the spacing of measurement sensors generating feedback signals. In this article, the application of the LQR algorithm to the node displacement control in a spatial truss has been presented. The spacing of active members in the truss structure on the basis of the force distribution in the truss members has been suggested.

Keywords: *piezoelectric, truss, actuator, LQR control*

STEROWANIE LQR PRZEMIESZCZENIAMI WĘZŁÓW PRZESTRZENNEJ KRATOWNICY Z AKTYWNYMI PRĘTAMI PIEZOELEKTRYCZNYMI

Zdolność tłumienia drgań jest wymagana w wielu konstrukcjach, których jednym z elementów są kratownice. Zwiększenie tłumienia drgań kratownicy jest możliwe za pomocą metod biernych lub przez zastosowanie aktywnego układu sterowania drganiami, zintegrowanego z konstrukcją kratownicy. Układ sterowania może oddziaływać na konstrukcję kratownicy przez specjalnie zaprojektowane aktuatory, które generują siły aktywnej regulacji w odpowiednio wybranych węzłach kratownicy. Piezoelektryki są materiałami, które mogą być wykorzystane do budowy takich aktuatorów. Projekt układu sterowania obejmuje konstrukcję aktywnego pręta kratownicy, rozmieszczenie aktywnych prętów w strukturze kratownicy, opracowanie algorytmu sterowania oraz rozmieszczenie czujników pomiarowych, generujących sygnały sprzężenia zwrotnego. W artykule przedstawiono zastosowanie algorytmu LQR w sterowaniu przemieszczeniami węzłów przestrzennej kratownicy oraz zaproponowano rozmieszczenie aktywnych prętów w strukturze kratownicy na podstawie rozkładu sił w prętach kratownicy przy występowaniu zakłóceń zewnętrznych.

Słowa kluczowe: *piezoelektryk, kratownica, aktuator, sterowanie LQR*

1. INTRODUCTION

The ability to damp vibration is required in many applications of truss structures. It is possible to reduce the nodal displacements of trusses by passive means, but this is achieved at the cost of increasing its mass. In some structures, for example in spacecraft structures, this is an important disadvantage. Hence the application of smart materials and a suitable control system is a promising direction of scientific research in this field. Smart materials are materials the static and dynamic characteristics of which can be controlled. The trusses, in which such material is implemented, are called smart trusses.

Piezoelectric materials can be used in a vibration damping system. The conversion from electrical energy to mechanical energy (converse piezoelectric effect) is used to generate a force by actuators in the active system for the suppression of the truss vibration. Actuators are the main part of the truss active members, several structures of which are presented in the scientific papers (Anderson 1990, Li 1998, Zheng 2008). The conversion from mechanical energy to electrical energy (the direct piezoelectric effect) is used in the measurement of the output values, for example the accelerations of the selected truss nodes (Song 2001).

A spatial truss with active members is a MIMO control object. The control algorithms designed in the state space can be used for such objects. In the literature, several algorithms are presented in this field: LQR (Bueno 2008), LQG (Wagner 2005), H_2 (Abreu 2010), H_∞ (Carvalhal 2005). One of the algorithms, most often used is the LQR. The mathematical model of the application of the LQR controller for 2D truss is presented in (Kwon 1997). The results of the laboratory research of the LQR control system for a simple 3D truss is described in (Bueno 2008). The maintenance of the initial positions of the nodes of the truss is the main task in control systems with the LQR algorithm presented in the literature. The initial positions of the nodes are the positions before the appearance of the external force effects e.g. displacements of

* AGH University of Science and Technology, Faculty of Mechanical Engineering and Robotics, Department of Process Control, Krakow, Poland; dariusz.grzybek@agh.edu.pl

truss nodes caused by the action of the wind. In other words, the task of the control system is the minimization of such effects. Such a steering task causes the design of the LQR control with a constant support in the feedback loop. Such algorithms are generally useful only for systems, in which output variables do not track the inputs. Hence, control systems in the state space are designed without a set value.

The spacing of active members in a truss structure is a difficult issue. In the literature, several methods are presented: based on the distribution of the modal strain energy (Preumont 1992), the minimization of optimal index (Lu 1992), Simulated Annealing (Yang 2005) and Genetic Algorithm (Degertekin 2007).

In this paper, the spacing of active members is defined on the basis of the force distribution in passive members. The active members were introduced to the truss structure in place of the passive members in which the highest compressive forces appeared.

2. MATHEMATICAL MODEL OF THE TRUSS

The equation of motion of the truss has the following form (Lewandowski 2006):

$$\boldsymbol{M}\,\ddot{\boldsymbol{q}}(t) + \boldsymbol{C}_d\,\dot{\boldsymbol{q}}(t) + \boldsymbol{K}_s\,\boldsymbol{q}(t) = \boldsymbol{E}\,\boldsymbol{u}(t) + \boldsymbol{p}(t) \tag{1}$$

where: $\boldsymbol{q}$ is the vector of the truss nodal displacements, $\boldsymbol{u}$ is the vector of control signals, $\boldsymbol{p}$ – the vector of disturbances, $\boldsymbol{M}$ is the mass matrix, $\boldsymbol{C}_d$ is the damping matrix, $\boldsymbol{K}_s$ is the stiffness matrix, $\boldsymbol{E}$ is the matrix of control signal locations in the truss structure. Matrix $\boldsymbol{C}_d$ was calculated from the dependence (Lewandowski, 2006):

$$\boldsymbol{C}_d = \alpha\boldsymbol{M} = 2\gamma\omega\boldsymbol{M} \tag{2}$$

where: γ is the damping coefficient, ω is the natural frequency of the truss. The constant value of the damping coefficient was assumed in the calculation (γ = 0,01) and the first natural frequency of the modelled truss was chosen (ω = 203.8 rad/s).

The state space model of the truss is given by:

$$\begin{cases} \dot{\boldsymbol{x}}(t) = \boldsymbol{A}\boldsymbol{x}(t) + \boldsymbol{B}\boldsymbol{u}(t) + \boldsymbol{H}\boldsymbol{p}(t) \\ \boldsymbol{y}(t) = \boldsymbol{C}\boldsymbol{x}(t) \end{cases} \tag{3}$$

where: $\boldsymbol{x}$ is the state vector, $\boldsymbol{u}$ is the control signal vector, $\boldsymbol{p}$ is the disturbance vector, $\boldsymbol{y}$ is the output vector, $\boldsymbol{A}$ is the state matrix, $\boldsymbol{B}$ is the control matrix, $\boldsymbol{H}$ is the disturbance matrix, $\boldsymbol{C}$ is the output matrix. Matrices $\boldsymbol{A}$, $\boldsymbol{B}$, $\boldsymbol{H}$ can be calculated using the following expressions:

$$\boldsymbol{A} = \begin{bmatrix} \boldsymbol{0} & \boldsymbol{I} \\ -\boldsymbol{M}^{-1}\boldsymbol{K}_s & -\boldsymbol{M}^{-1}\boldsymbol{C}_d \end{bmatrix} \quad \boldsymbol{B} = \begin{bmatrix} \boldsymbol{0} \\ \boldsymbol{M}^{-1}\boldsymbol{E} \end{bmatrix} \quad \boldsymbol{H} = \begin{bmatrix} \boldsymbol{0} \\ \boldsymbol{M}^{-1} \end{bmatrix} \tag{4}$$

3. MATHEMATICAL MODEL OF THE PIEZOELECTRIC ACTUATOR

For control purposes, some of the passive members in the truss were replaced by the active members made of piezoelectric material. The structure of an active member is presented in figure 1.

The basic part of the active member consists of piezoelectric material, which generates a force on the principle of the inverse piezoelectric effect. A piezoelectric stack was assumed in the simulation research. The structure of a piezoelectric stack is shown in figure 2.

The basic equations describing electromechanical conversion in the piezoelectric material are given by (Nye 1957, IEEE 1987):

$$\begin{aligned} S_{ij} &= s_{ijkl}^{(E)} T_{kl} + d_{kij} E_k \\ D_i &= d_{ikl} T_{kl} + \varepsilon_{ik}^{(T)} E_k \end{aligned} \quad \text{for} \quad i, j, k, l = 1, 2, 3 \tag{5}$$

where: S is the strain tensor, T is the stress tensor, D_i are the components of the electric induction vector, E_k – the components of the electric field intensity vector, s is the compliance tensor (m^2N^{-1}), d is the electromechanical coupling tensor (CN^{-1}), ε is the permeability tensor (Fm^{-1}). Equations (5) can be written using the matrix notation as follows:

$$\begin{aligned} S_p &= s_{pq}^{(E)} T_q + d_{pk} E_k \\ D_i &= d_{iq} T_q + \varepsilon_{ik}^{(T)} E_k \end{aligned} \quad \text{for} \quad i, k = 1, 2, 3, \quad p, q = 1, \ldots, 6 \tag{6}$$

The relationship between electrical and mechanical variables is given by the following formulas (Lefeuvre 2006):

$$E(t) = -\frac{V_p(t)}{L} \quad S(t) = \frac{\Delta L(t)}{L}$$

$$I_p = A\frac{dD(t)}{dt} \quad F_p(t) = AT(t) \tag{7}$$

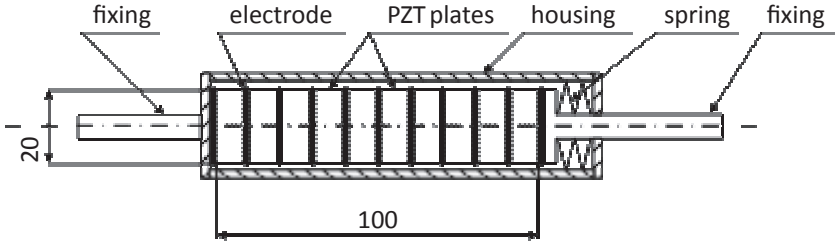

Fig. 1. The active member structure

where: V_p is the supplied voltage (V), L is the thickness of the piezoelectric plate (m), I_p is the current (A), F_p is the force generated by the piezoelectric plate (N), ΔL is the elongation of the piezoelectric plate (m), A is the area of the piezoelectric plate (m^2).

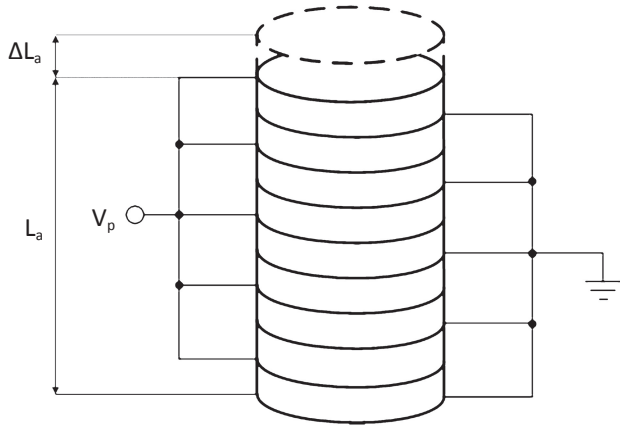

Fig. 2. The piezoelectric stack structure

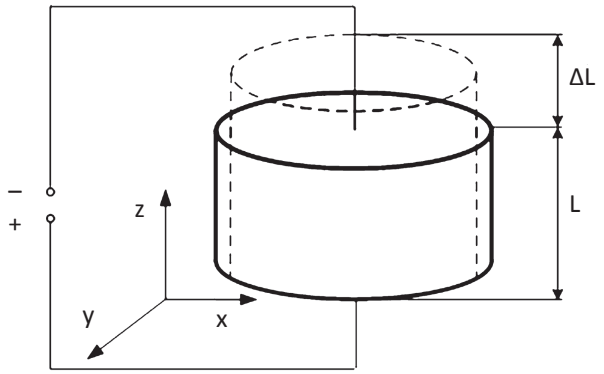

Fig. 3. The denotation of the axes

Assuming that the axes are denoted as shown in figure 3, the following equations are obtained from Eq. (6):

$$S_3 = s_{33}^{(E)} T_3 + d_{33} E_3$$
$$D_3 = d_{33} T_3 + \varepsilon_{33}^{(T)} E_3 \tag{8}$$

Introducing expressions (7) into the first equation in (8) one obtains:

$$V_p(t) = \frac{L s_{33}^{(E)}}{d_{33} A} F_p(t) - \frac{A}{d_{33}} \Delta L(t) \tag{9}$$

The supplied voltage V_p is used for the generation of the force F_p as well as elongation ΔL. If the piezoelectric plate cannot expand, all the supplied voltage is converted to the force.

The force F_p generated by the piezoelectric stack, assuming that $\Delta L=0$, is given by:

$$F_p(t) = \frac{d_{33} A n}{s_{33}^{(E)} L_a} V_p(t) = \alpha V_p(t) \tag{10}$$

where: n is the number of piezoelectric plates in the actuator, L_a is the length of the piezoelectric stack, α is the proportionality coefficient (NV^{-1}). On the basis of the material data from Morgan Technical Ceramics Company, the ratio of $d_{33}/ s_{33}^{(E)}$ was calculated for several types of Lead Zirconate Titanate ceramics (PZT). Table 1 gives the values of this coefficient.

PZT5K1 ceramic has been chosen for the simulation studies discussed below. The basic dimensions of the piezoelectric stack are as follows: L_a = 0.1 m, A = 3.14·10^{-4} m^2, the number of the plates n = 10. For these data the proportionality coefficient α = 1.33 NV^{-1}.

4. LQR CONTROL ALGORITHM

Control signal $\boldsymbol{u}$ in the LQR control system can be expressed as follows (Ogata 2008):

$$\boldsymbol{u}(t) = \boldsymbol{R}^{-1} \boldsymbol{B}^T \boldsymbol{P} \boldsymbol{x}(t) = -\boldsymbol{K} \boldsymbol{x}(t) \tag{11}$$

where $\boldsymbol{P}$ is a symmetrical semipositive-definite solution of the Riccati equation, $\boldsymbol{K}$ is a matrix of the gains in the controller feedback. $\boldsymbol{K}$ is calculated by the minimization criterion:

$$J = \int_0^\infty \left(\boldsymbol{x}^T(t) \boldsymbol{Q} \boldsymbol{x}(t) + \boldsymbol{u}^T(t) \boldsymbol{R} \boldsymbol{u}(t) \right) dt \tag{12}$$

where $\boldsymbol{Q}$ is a positive definite or semidefinite weighting matrix, $\boldsymbol{R}$ is a positive definite weighting matrix. The block diagram of LQR control is presented in figure 4.

Table 1

Properties of the selected PZT ceramics

Ceramics	Unit	PZT5A1	PZT5A2	PZT5A3	PZT5A4	PZT5J1	PZT5H1
$d_{33}/s_{33}^{(E)}$	Cm^{-2}	23.77	19.89	19.89	25.55	22.02	28.31
Ceramics	Unit	PZT5H2	PZT503	PZT504	PZT507	PZT508	PZT5K1
$d_{33}/s_{33}^{(E)}$	Cm^{-2}	28.50	27.77	23.68	41.00	32.72	42.64

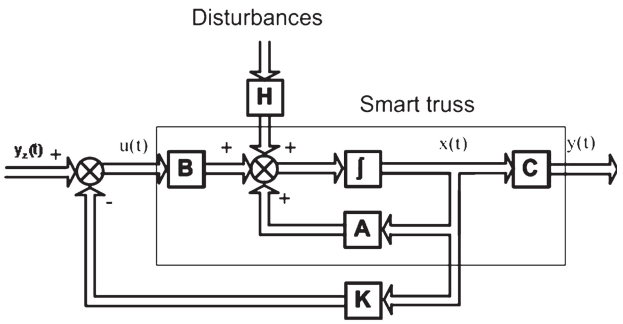

Fig. 4. The diagram of the LQR algorithm for the smart truss

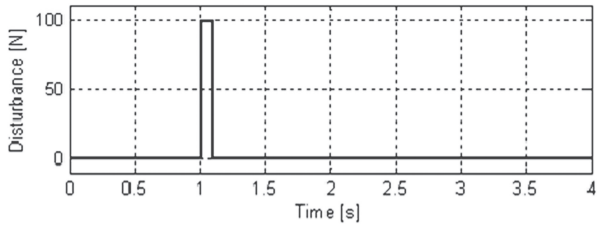

Fig. 5. The value of the simulated disturbance

5. RESULTS OF THE SIMULATIONS

5.1. The structure of the simulated truss

The truss is a 3D structure with 36 degrees of freedom and is 0.75 m high and 0.25 m wide. The structure consists of 42 passive members and 16 nodes. The passive members are made of steel and have a circular cross-section. The truss is statically determined:

$$n_{pm} = 3 \times n_n - 6 \Rightarrow 42 = 3 \times 16 - 6 \tag{13}$$

where: n_{pm} is the number of the passive members, n_n is the number of the nodes. For this truss, the dependence (1) contains 36 differential equations. Matrices $\boldsymbol{M}$ and $\boldsymbol{K}_s$ were generated in the ANSYS program on the basis of the model of the truss shown in figure 7, for the values of truss parameters in table 2. In the simulation studies, the nodes were not modelled.

Table 2

Values of the basic truss parameters

Quantity	Symbol	Value	Units
Length of member located along axes: *x, y, z*	l_m	0.25	m
Length of diagonal member	l_{md}	0.35	m
Diameter of member	Φ_m	0.005	m
Young's modulus	E	$205 \cdot 10^9$	Pa
Poisson's ratio	ν	0.3	–
Density of steel	ρ	7850	kg/m^3

5.2. The spacing of active members

In order to find the spacing of the active members, the simulation studies have been conducted for the external disturbance $P_z(t)$, shown in figure 5.

Four cases of the disturbance locations have been simulated:

location no a: disturbance $P_z(t)$ affecting nodes no. 13 and 16 along the *x* axis (fig. 6a),
location no b: disturbance $P_z(t)$ affecting nodes no. 14 and 15 along the *x* axis (fig. 6b),
location no c: disturbance $P_z(t)$ affecting nodes no. 13 and 14 along the *z* axis (fig. 6c),
location no d: disturbance $P_z(t)$ affecting nodes no. 15 and 16 along the *z* axis (fig. 6d).

The deformation of truss corresponding to the external disturbances of figure 6 are presented in figure 7.

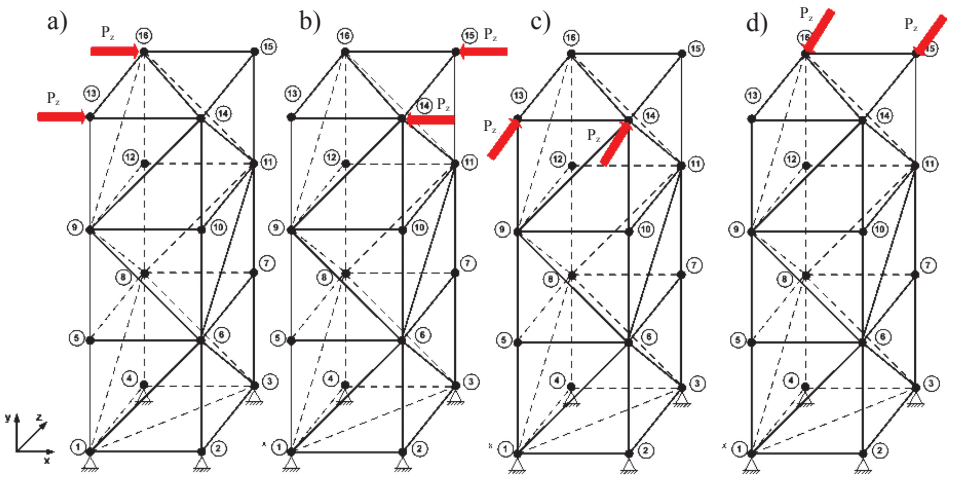

Fig. 6. The simulated disturbances used during the stage of the active member placement

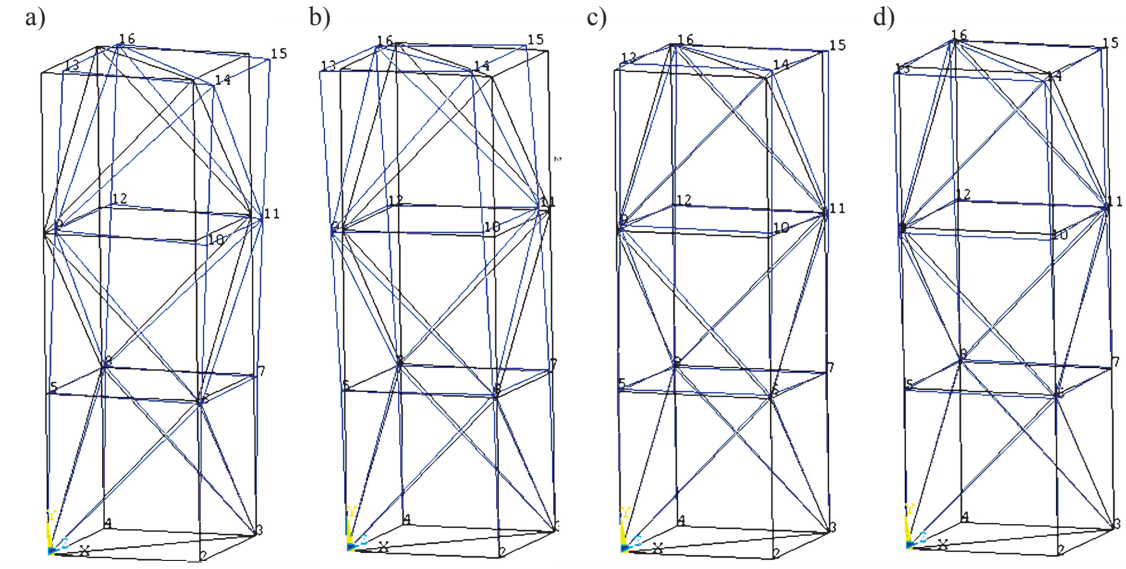

Fig. 7. The deformation of the truss structure: black lines – shape before the application of force, blue lines – shape after force excitation

Table 3

Values of the five highest compressing stresses

No	Location of the disturbances	No[-]/ value [MPa]	No[-]/ value [MPa]	No[-]/ value [MPa]	No[-]/ value [MPa]	No[-]/ value [MPa]
1.	at nodes no 13 and 16 along *x* axis	6/15.27	7/10.18	15/10.18	32/7.20	34/7.20
2.	at nodes no 14 and 15 along *x* axis	8/15.27	5/10.186	13/10.18	30/7.20	36/7.20
3.	at nodes no 13 and 14 along *z* axis	8/15.27	7/10.18	15/10.18	31/7.20	37/7.20
4.	at nodes no 15 and 16 along *z* axis	6/15.27	5/10.18	13/10.18	33/7.20	35/7.20

The values of the highest compressive stress for all the cases are presented in table 3.

Two passive members with the highest compressive stresses along the *y* axis were selected: no. 6, and 8, as well as two passive diagonal members: no. 30 and 32. These passive members were replaced by active members. The spacing of the active members in the truss structure is presented in figure 8.

The state-space model of the truss with the active members is given by:

$$\begin{cases} \dot{\boldsymbol{x}}(t) = \boldsymbol{A}_a\boldsymbol{x}(t) + \boldsymbol{B}_a\boldsymbol{u}(t) + \boldsymbol{H}\boldsymbol{p}(t) \\ \boldsymbol{y}(t) = \boldsymbol{C}\boldsymbol{x}(t) \end{cases} \tag{14}$$

where: matrix $\boldsymbol{A}_a$ is the same as $\boldsymbol{A}$ on the basis of the assumption that the stiffness and the mass of an active member are the same as the stiffness and the mass of a passive member, matrix $\boldsymbol{B}_a$ is calculated (equation 4) with the use of a new matrix $\boldsymbol{E}$ containing additional four columns corresponding to the four active members.

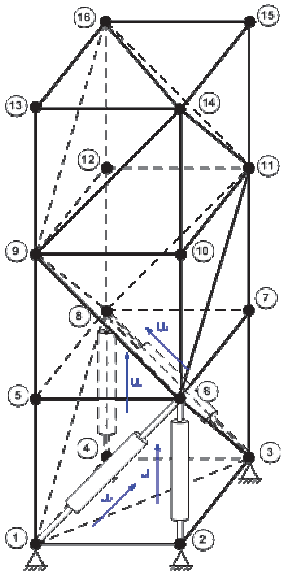

Fig. 8. A sketch of the placement of the active members inside the truss structure

5.3. LQR control system

The basic assumptions used are as follows:

a) *The weighting matrix* $\boldsymbol{Q}$ has been assumed in the following from (Lewandowski 2006):

$$\boldsymbol{Q} = \begin{bmatrix} \boldsymbol{K}_s & 0 \\ 0 & \boldsymbol{M} \end{bmatrix} \tag{15}$$

b) *The weighting matrix* $\boldsymbol{R}$ is given by (Brzózka 2004):

$$\boldsymbol{R} = \boldsymbol{diag}\left(r_{11}, r_{22}, r_{33}, r_{44}\right) \tag{16}$$

with:

$$r_{11} = \frac{1}{u_{1max}^2}, r_{22} = \frac{1}{u_{2max}^2}, r_{33} = \frac{1}{u_{3max}^2}, r_{44} = \frac{1}{u_{4max}^2} \tag{17}$$

where: u_{1max}, u_{2max}, u_{3max}, u_{4max} are the maximum values of the control signals. On the basis of the material data from Morgan Technical Ceramics Company, these maximum values have been assumed as follows: $u_{1max} = u_{2max} = u_{3max} = u_{4max} = 300$ V. Hence:

$$\boldsymbol{R} = 1{,}11 \times 10^{-5} \cdot \boldsymbol{I}_{4x4} \tag{18}$$

c) *The output signal* is the displacement of node no 16 along the x axis.

d) *The set value* is equal to 0.

e) *The disturbances* are presented in figure 9:
- location no. 1: fig. 9a,
- location no. 2: fig. 9b,
- location no. 3: fig. 9c.

5.4. Simulation results

The simulation studies have been conducted in the MATLAB/Simulink program. The optimum gain matrix $\boldsymbol{K}$ was calculated using the *lqr function* from the MATLAB program. $\boldsymbol{K}$ is given by:

$$\boldsymbol{K} = \begin{bmatrix} k_{11} & k_{12} & \dots & k_{1n} \\ k_{21} & k_{22} & \dots & k_{2n} \\ k_{31} & k_{32} & \dots & k_{3n} \\ k_{41} & k_{42} & \dots & k_{4n} \end{bmatrix} \quad \text{for } n = 72 \tag{19}$$

The following exemplary values of the elements of the $\boldsymbol{K}$ have been obtained: $k_{11} = -3075700$, $k_{12} = -6651000$, $k_{13} = -1536800$, $k_{14} = 1590200$.

The results of the application of the LQR control system with four active members generating an additional force having an effect on nodes no. 6, and no. 8 are presented in figure 10 and 11.

The displacements of node no. 16 are shown in figure 10.

The control signals are presented in figure 11.

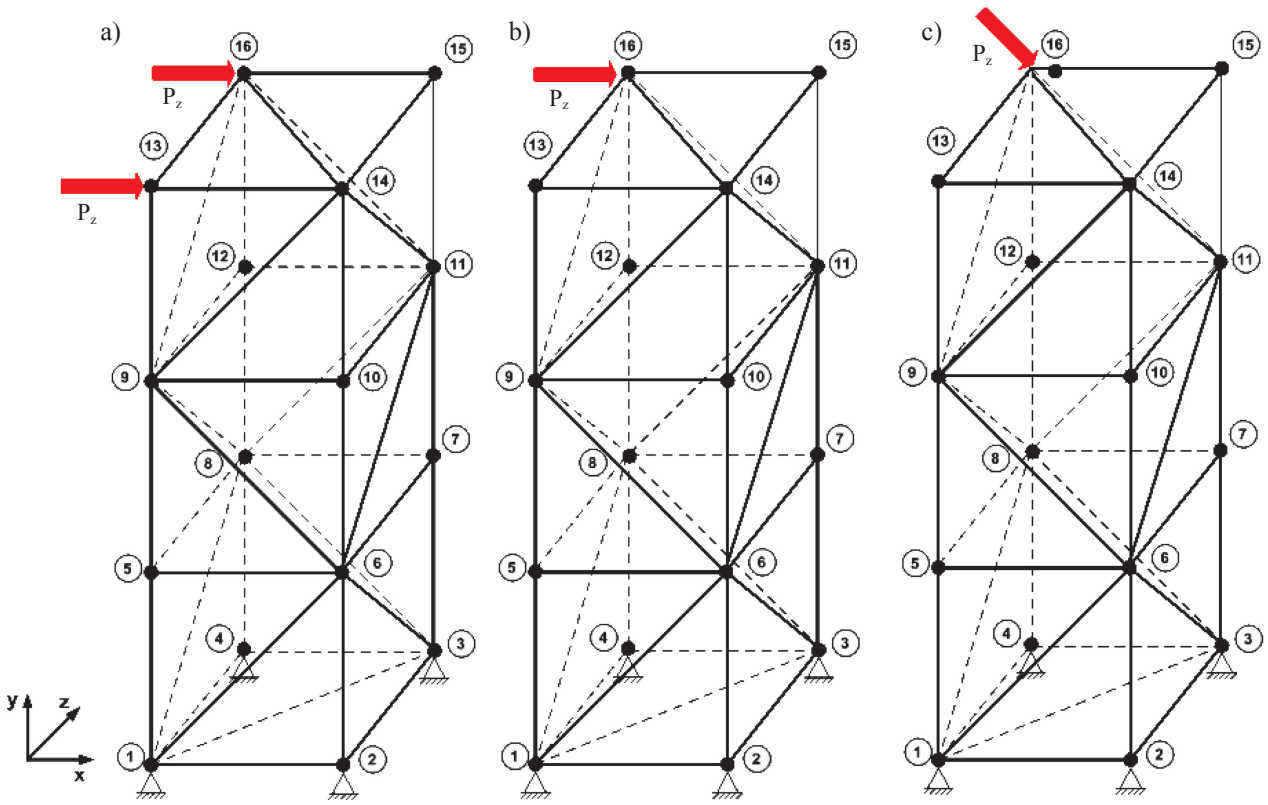

Fig. 9. The disturbances used in the simulation studies

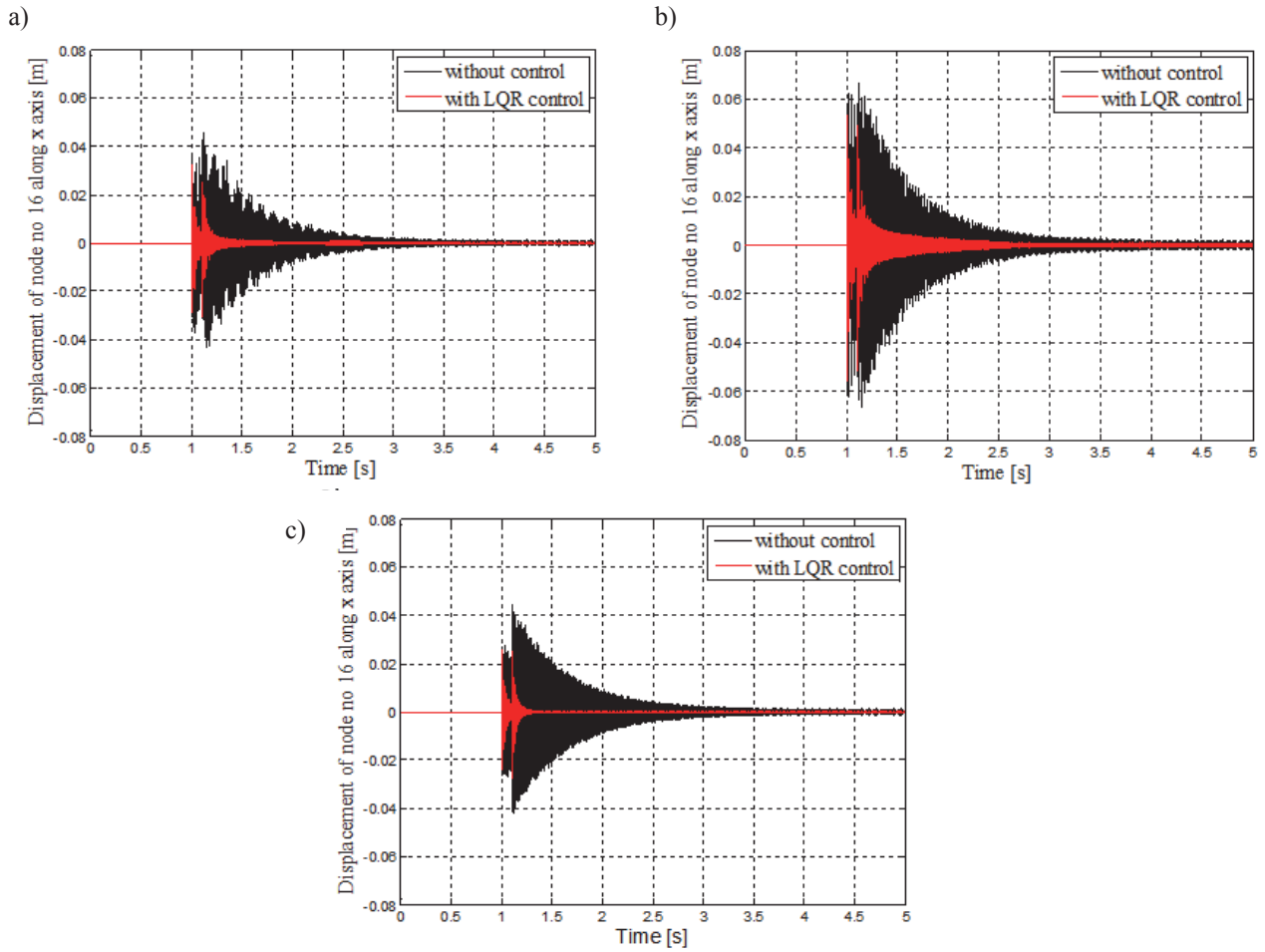

Fig. 10. The results of the simulation studies: the displacements of the node no. 16 along the x axis a) for the disturbance location no. 1, b) for the disturbance location no. 2, c) for the disturbance location no. 3

6. CONCLUSIONS

On the basis of the simulation studies, the selected results of which were described in the previous chapter, the following conclusions can be established:

a) For the assumed criterion of control quality, which was the smallest possible displacement of node no. 16 along the *x* axis, the best spacing of the active members was selected (fig. 8). This spacing was chosen on the basis of the force distribution in the truss members. The passive members (no. 6 and no. 8), in which the highest compressing forces appeared along the *y* axis for the disturbances presented in figure 6, were replaced by active members containing a piezoelectric actuator. In the diagonal members, the highest compressive forces appeared in members no. 30, 31, 32, 33. On the basis of the simulation results, members no. 30 and 32 were selected and were replaced by active members. During simulations, some other spacing patterns were also verified, but the simulated displacements of node no. 16 for them were higher than the simulated displacements for the spacing presented in figure 10. The general conclusion is that the replacement of the members with the highest compressive forces by active members enables effective control of a smart truss.

b) The active members installed in the smart truss should be fixed to the truss support, embedded in the ground or another structure. The best control results were obtained for such a spacing. The installation of one active member without the connection with the truss support causes the generation of two control signals of the same value and these signals affect two nodes, but the effect of this control is opposite.

c) The weights in the matrixes $\boldsymbol{Q}$ and $\boldsymbol{R}$ are important factors influencing the control signals generated by the LQR controller. The designer of the control system should provide adequate $\boldsymbol{Q}$ and $\boldsymbol{R}$ matrices. In the simulations $\boldsymbol{Q}$ was a matrix containing matrices $\boldsymbol{M}$ and $\boldsymbol{K}_s$. $\boldsymbol{R}$ was a diagonal matrix with the weight of $1.11 \cdot 10^{-5}$. These values allowed to reach high control efficiency.

The study is completed under the AGH-UST's research program No 11.11.130.560 sponsored by statutory research funds. AGH University of Science and Technology, Faculty of Mechanical Engineering and Robotics, Department of Process Control.

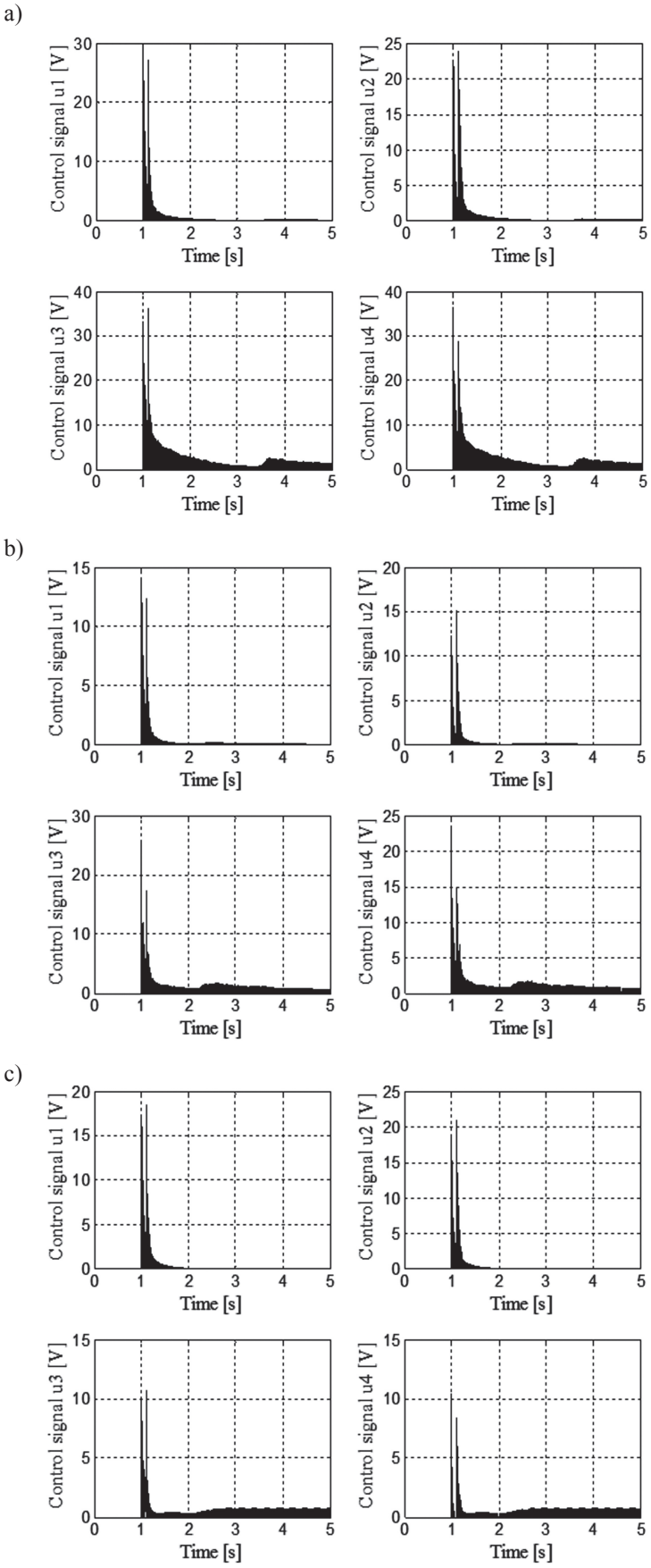

Fig. 11. The control signals in the simulation research: a) for the disturbance location no. 1, b) for the disturbance location no. 2, c) for the disturbance location no. 3

References

Abreu G.L.C., Lopes V. 2010, *H_2 Optimal control for smart truss structure*, Proceedings of the 9th Brazilian Conference on Dynamics Control and their Applications, pp. 961–966

Anderson E.H., Moore D.M., Fanson J.L. 1990, *Development of an active truss element for control of precision structures*, Optical Engineering, vol. 29, pp. 1333–1341

Brzózka J. 2004, *Regulatory i układy automatyki*, Wydawnictwo Mikom, Warszawa

Bueno D., Marqui C., Santos R., Neto C., Lopes V. 2008, *Experimental active vibration control in truss structures considering uncertainties in system parameters*, Mathematical Problems in Engineering, doi:10.1155/2008/754951

Carvalhal R., Silva S., Lopes V. 2005, *Robust Control Applications for Smart Truss Structure*. Conference & Exposition on Structural Dynamics

Degertekin S.O. 2007, *A comparison of simulated annealing and genetic algorithm for optimum design of nonlinear steel space frames*, Structural and Multidisciplinary Optimization, vol. 34, pp. 347–359

Kwon Y.W., Bang H. 1997, *The finite element method using MATLAB*, CRC Press, Washington

Lefeuvre E., Badel A., Richard C., Petit L., Guyomar D. 2006, *A comparison between several vibration-powered piezoelectric generators for standalone systems*, Sensors and Actuators 2006, no 126, pp. 405–416

Lewandowski R. 2006, *Dynamika konstrukcji budowlanych*, Wydawnictwo Politechniki Poznańskiej, Poznań

Li J.-B., Xiong Sh.-B. 1998, *Experimental studies of vibration control of a space truss structure*, Proceedings of the 16th International Modal Analysis Conference, vol. 3243

Lu L-Y, Utku S., Wada B.K. 1992, *On the placement of active members in adaptive truss structures for vibration control*, Smart Material and Structure, no 1, pp. 8–23.

Nye J.F., 1957, *Physical properties of crystals*, Oxford at the Clarendon Press, Oxford

Ogata K. 2008, *MATLAB for control engineers*, Upper Saddle River, New Jersey

Preumont A., Dufour J.P., Malekian C. 1992, *Active damping by a local force feedback with piezoelectric actuators*, Journal of Guidance, Control and Dynamic, vol. 15, pp. 390–395

Song G., Vlattas J., Johnson S.E., Agraval B.N. 2001, *Active vibration control of a space truss using a lead zirconate stack actuator*, Proceedings of the Institution of Mechanical Engineers, vol. 215, pp. 355–361

Standards Committee of the IEEE Ultrasonics, Ferroelectrics, and Frequency Control Society, Air American National Standard 1987, *IEEE Standard on Piezoelectricity*, The Institute of Electrical and Electronics Engineers, New York

Wagner M., Grillenbeck A., Abou-El-Ela A. 2005, *Active vibration suppression in spacecraft structures based on LQG-Controller and Kalman-Observer*, Proceedings of the European Conference on Spacecraft Structures, Materials and Mechanical Testing

Yang F., Sedaghati R. 2005, *Optimal Placement of Active Bars in Smart Structures*, Proceedings of the IEEE International Conference on Mechatronics & Automation

Zheng K., Zhang Y., Yang Y., Yan S., Dou L., Chen J. 2008, *Active vibration control of adaptive truss structure using fuzzy neutral network*, Proceedings of Chinese Control and Decision Conference